

Study of Lithium Battery Thermal Effect on Battery and Hybrid Battery/Ultra-Capacitor Sizing for an Electric Vehicle

Masoud Masih-Tehrani and Rambod Yahyaei

Vehicle Dynamical Systems Research Laboratory, School of Automotive Engineering, Iran University of Science and Technology, Tehran, Iran

Abstract: A thermal-based cost function is proposed to optimize the lithium battery size of an electric vehicle (conventional battery-based energy storage system or hybrid battery/ultra-capacitor energy storage system) in this paper. The proposed cost function is determined the battery lifetime with considering both the battery current and battery temperature, besides the overall cost of energy storage system. The studied energy storage systems are a conventional battery-based energy storage system and a hybrid energy storage system (HESS) (battery/ultra-capacitor). In HESS case, the effect of ultra-capacitor (UC) adding is moderating the battery current directly and battery temperature indirectly. The constraints of the optimum energy storage system sizing problem are the vehicle performance (e.g., driving cycle tracking and vehicle range). In this paper As a case study, an electric motorcycle modeled. The results show battery sizing should be redesign when the battery thermal model consider. Also, battery life decreases, and a battery temperature rise and when the ambient temperature growth, vehicle range increases. On the other hand, a lighter and cheaper cooling system could use in HESS in comparison with the ESS. Finally, the battery life improvement for a HESS is more noticeable when the battery thermal model used as compared with the case that the battery thermal model is disabled.

Keywords: Lithium battery thermal model, Hybrid Energy Storage System, Battery sizing, Electric motorcycle

1. Introduction

Energy wasting is an important issue in the vehicle [1]. Electric and hybrid vehicles [2] are an attractive research subject in the last decades [3], because of efficiency and the regenerative braking ability. The battery, as the energy storage system (ESS) of an electric vehicle, is a significant component of the EV [4]. A high portion of the EV cost is related to the battery cost [5]. Also, the battery life is finite, and it should be replaced after degradation [6]. Therefore, proper battery sizing and systematic design can improve the cost advantages of the EV [7].

For a cell sizing process, the vehicle powertrain model and a precise battery model are used. There are some EV powertrain models are developed recently, such as ADVISOR [8] and AVL/CRUISE [9]. In this paper, the package of Esfahanian et al. [10] is utilized for powertrain modeling. A famous and efficient approach to dynamical battery modeling is equivalent circuit [11]. On the other hand, many of the proposed battery models do not have a thermal model [12] (they are temperature independent); while the thermal model has a significant effect on the battery behavior [13] and maybe cause to explosion hazards (because of the thermal runaway phenomenon) [14]. Battery heat produced during the vehicle driving cycles should be handled to keep battery cell performance and good lifetime [15]. On the other hand, the effect of temperature on the fulfillment of a system is also proofed in many applications, such as the catalyst of a four-stroke engine [16].

Nelson et al. studied on the battery sizing for a plug-in hybrid electric vehicle [17]. They to look at the price for the thermal management system and increase battery lifetime investigate the effect of the designed system. However, the thermal model was not at the core of the battery sizing process [17]. Correa et al. developed a sizing method for the battery in a fuel cell vehicle. They did not concentrate on the battery temperature in their sizing process [18]. Colzi et al. proposed three items for battery sizing for a range

extender electric vehicle: “mean daily traveled distance,” “total-life battery range,” and “the satisfaction of the worst-case”. They did not mention the battery thermal behavior [19].

Hybrid energy storage systems (HESS) are introduced from 1989 [20] and they attracted considerable attention. Fig1 shows the paper trends about the HESS (with these keywords: “Hybrid Energy Storage,” “Hybrid Power Systems,” “Hybrid Energy System,” “Hybrid Energy Storage Systems”), which is indexed from 1987 until now, in “scopus.com.” This figure presents the high attention to this subject in the last decade.

Wu et al. worked on a hybrid solar-battery design and management [21]. Ruiz-Cortes et al. studied on the HESS for residential application [22]. Bartholomäus et al. proposed a Model predictive control for power-sharing between battery and supercapacitor in a HESS [23]. In these works and much same as them, the battery temperature and thermal behavior are not determined in the HESS sizing and control design process.

In this paper, the combination of battery and UC is assumed as the HESS [24]. The primary target of this arrangement is to moderate the battery current to improve the battery lifetime [25]. An unaware point about HESS is that the battery current reduction can reduce the battery temperature and improve the battery thermal (cooling) system. Therefore, the battery lifetime maybe increases due to the lower battery temperature, in addition to the effect of the lower battery current.

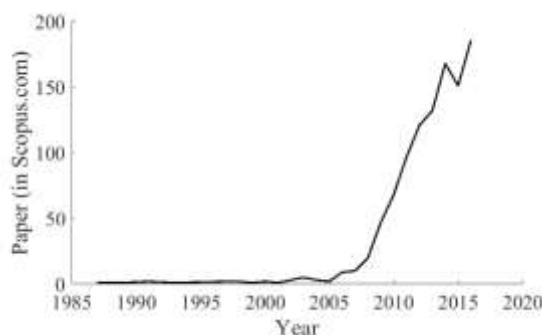


Fig1. HESS paper trends (in scopus.com)

The next section is about lithium battery modeling, especially about battery thermal model. In section 3, the case study of this paper will be introduced In this article; an electric motorcycle is investigated in the FTP driving cycle. After that, the HESS modeling and sizing will be discussed.

2. Lithium battery modeling

The lithium battery model consists of an equivalent electrical circuit, which has a dynamic model of this energy storage system. The lithium battery model is implemented in MATLAB/Simulink software (Fig2).

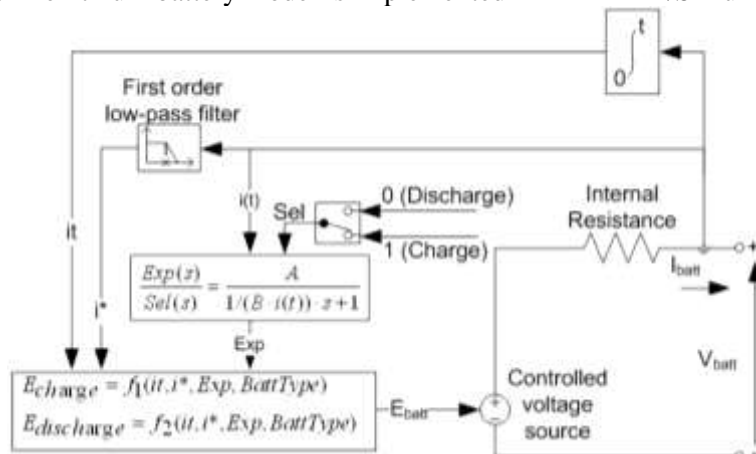


Fig2. Lithium battery dynamic model in MATLAB/Simulink [26]

The equations of Fig2 are as follows [27]:

- Discharge model ($i^* > 0$):

$$f_1(it, i^*, i) = E_0 - K \cdot \frac{Q}{Q-it} \cdot i^* - K \cdot \frac{Q}{Q-it} \cdot it + A \cdot \exp(-B \cdot it) \quad (1)$$

○ Charge model ($i^* < 0$):

$$f_2(it, i^*, i) = E_0 - K \cdot \frac{Q}{it+0.1 \cdot Q} \cdot i^* - K \cdot \frac{Q}{Q-it} \cdot it + A \cdot \exp(-B \cdot it) \quad (2)$$

where:

- E_{batt} is nonlinear voltage (V).
- E_0 is constant voltage (V).
- K is polarization resistance (Ω).
- i^* is low-frequency current dynamics (A).
- i is battery current (A).
- it is extracted capacity (Ah).
- Q is maximum battery capacity (Ah).
- A is exponential voltage (V).
- B is exponential capacity (Ah^{-1}).

The battery model information is listed in Table 1. As seen in this Table, the model parameters of the LiFePO4 cell are determined by Omar et al. [28] (3rd column) and are scaled for the case study battery pack in the 4th column.

Table 1: Lithium battery (LiFePO4) parameters

Items	Units	Values for one LiFePO4 cell [28]	Values for battery pack (case study)
Nominal voltage	V	3.3	72.6
Rated capacity	Ah	2.3	33.8
Battery response time	s	30	30
Maximum capacity	Ah	2.3	33.8
Cut-off voltage	V	2.475	54.45
Fully charged voltage	V	3.748	82.456
Nominal discharge current	A	2.3	130.13
Internal resistance	Ω	0.014	0.0152
Capacity at nominal voltage	Ah	2.25	33.0652

The effect of temperature on the model parameters is represented by these equations [26].

○ Discharge model ($i^* > 0$):

$$f_1(it, i^*, i, T, T_a) = E_0(T) - K(T) \cdot \frac{Q(T_a)}{Q(T_a)-it} \cdot (i^* + it) + A \cdot \exp(-B \cdot it) \quad (3)$$

$$V_{batt}(T) = f_1(it, i^*, i, T, T_a) - R(T) \cdot i \quad (4)$$

○ Charge model ($i^* < 0$):

$$f_1(it, i^*, i, T, T_a) = E_0(T) - K(T) \cdot \frac{Q(T_a)}{it+0.1 \cdot Q(T_a)} \cdot i^* - K(T) \cdot \frac{Q(T_a)}{Q(T_a)-it} \cdot it + A \cdot \exp(-B \cdot it) \quad (5)$$

$$V_{batt}(T) = f_1(it, i^*, i, T, T_a) - R(T) \cdot i \quad (6)$$

$$E_0(T) = E_0|_{T_{ref}} + \frac{\partial E}{\partial T} (T - T_{ref}) \quad (7)$$

$$K(T) = K|_{T_{ref}} + \exp\left(\alpha \left(\frac{1}{T} - \frac{1}{T_{ref}}\right)\right) \quad (8)$$

$$Q(T_a) = Q|_{T_a} + \frac{\Delta Q}{\Delta T} \cdot (T_a - T_{ref}) \quad (9)$$

$$R(T) = R|_{T_{ref}} + \exp\left(\beta \left(\frac{1}{T} - \frac{1}{T_{ref}}\right)\right) \quad (10)$$

where:

- T_{ref} is nominal ambient temperature (K).
- T is the cell or internal temperature (K).
- T_a is ambient temperature (K).

- E/T is reversible voltage temperature coefficient (V/K).
- α is Arrhenius rate constant for the polarization resistance.
- β is Arrhenius rate constant for the internal resistance.
- $\Delta Q/\Delta T$ is maximum capacity temperature coefficient (Ah/K).

The cell or internal temperature, T , at any given time, t , is expressed as:

$$T(t) = L^{-1} \left(\frac{P_{loss} R_{th} + T_a}{1 + s \cdot t_c} \right) \quad (11)$$

where:

- R_{th} is thermal resistance, cell to ambient ($^{\circ}\text{C}/\text{W}$).
- t_c is the thermal time constant, cell to ambient (s).
- P_{loss} is the overall heat generated (W) during charge/discharge process and is given by

$$P_{loss} = (E_0(T) - V_{batt}(T)) \cdot i + \frac{\partial E}{\partial T} \cdot i \cdot T \quad (12)$$

The generalized life model as a function of the C-rate (ratio of the battery current to its capacity) is proposed by Wang et al. [29] as follows:

$$Q_{loss} = B \times \exp \left(-31,700 + 370.3 \times \frac{C-rate}{R \times T} \right) Ah^{0.55} \quad (13)$$

where Q_{loss} is the capacity loss in percent, B is the pre-exponential factor and is a function of $C-rate$ (Table 2), R is the gas constant, T is the absolute temperature, and Ah is the Ah-throughout which is expressed as $Ah = cycle\ number \times (DoD) \times (full\ cell\ capacity)$.

Table 2: Values of B with respect to the C-rate [29]

C-rate	C/2	2C	6C	10C
B Values	31630	21681	12934	15512

The life capacity (Ah) of the 2.6 Ah LiFePO4 battery cell for different battery currents are calculated using Equation (13). The life capacity is defined as the amount of capacity that the battery can provide at a particular current before its capacity reaches 20% [30].

The driving cycle capacity loss ($Q_{loss-DC}$) is given by Equation (4) [30].

$$Q_{loss-DC} = \sum \left(\frac{I_k \times \frac{it}{3600}}{LC(I_k)} \right), k = 0, 1, 2, \dots, t_{DC} \quad (14)$$

where I_k is the battery current at k th time step and k varies from zero to the driving cycle duration (t_{DC}). dt is the time step for the calculations and LC is the life capacity and is a function of I_k .

3. Case study (electric motorcycle)

As a case study, an electric motorcycle is examined in FTP driving cycle [31] (Fig3).

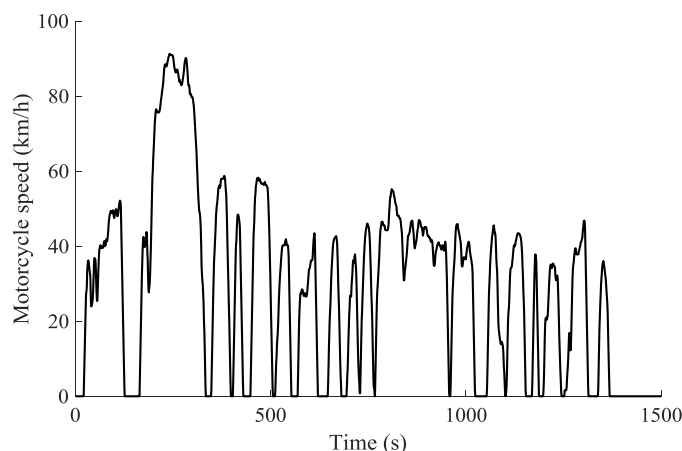


Fig3. FTP driving cycle (speed vs. time curve)

Main specifications and characteristics of the electric motorcycle and its powertrain are presented in tables 3 and 4, respectively.

Table 3: Electric motorcycle specifications

Items	Units	Values
Total mass (with driver)	kg	250
Rolling resistance coefficient	-	0.003
Drag coefficient	-	0.4
Frontal area	m ²	0.6
Tire radius	m	0.24

Table 4: Powertrain specifications of the electric motorcycle

System	Item	Units	Values
High voltage bus	Voltage	V	70
Traction motors	Power	kW	6 (peak 12)
	Torque	Nm	70 (peak 140)
Battery pack	Type	-	286 LiFePO4 cells (22 series 13 parallel)
	Voltage	V	72.6
	Capacity	Ah	33.8
	Cycle life	cycles	2000

The powertrain model is similar to the proposed models of Esfahanian et al. [10]. The performance of the designed battery pack is listed in Table 5. In this calculation, the thermal model of battery is neglected, and the battery temperature is assumed 25°C (for battery life determination). As seen in this table, the driving cycle tracking error is very low, and the vehicle range is about 100 km (acceptable). The number of the parallel battery (capacity) can be resized to adopt the vehicle range and battery life. It is evident that if the battery capacity is rising, the vehicle (motorcycle) range would be increased. However, the added weight of the bigger battery maybe hurt the vehicle range. On the other hand, the larger battery has a lower *C – rate* with a specific battery current; therefore, the battery life would be increased. Because of the battery life is lower than 10 years, the battery should be replaced one time and the overall cost of the battery is twice of the initial battery cost.

Table 5: The performance of the designed battery pack without thermal model in 25°C

Tracking error (km/h)	Vehicle range (km)	Initial cost (USD)	Battery life (year)	10-year overall cost (USD)
0.18	99.23	1250	6.08	2500

If the performance of Table 5 is recalculated in other ambient temperature, three first columns of that table are not varied (the thermal model is not activated). Fig4 shows the battery life and overall cost vs. ambient temperature for the designed battery pack without a thermal model. As shown in this figure, in a warm environment (more than 25°C), the 10-year overall battery cost would be greater than 2500 USD, because the battery life is lower than five years and the battery replacement exceeds one time during ten years.

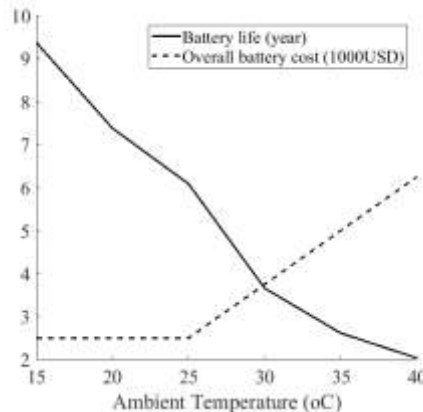


Fig4. Battery life and overall cost vs. ambient temperature for the designed battery pack without thermal model

Battery current, battery temperature and battery life loss for 13 parallel battery pack, with and without battery thermal models are shown in Fig5. As presented here, the battery current for both models is very similar. However, the battery temperature of the battery thermal model is higher than of the battery model without thermal modeling. Therefore, the battery life loss (down figure) of the battery with the thermal model is greater than another model.

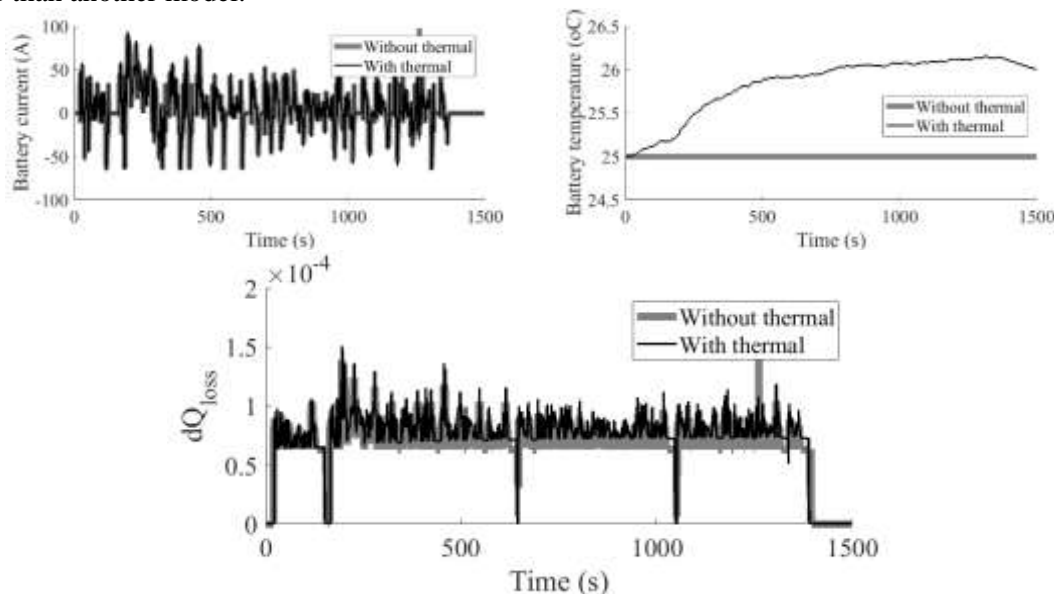


Fig5. Battery current (up left figure), battery temperature (upright figure) and battery life loss (down figure) for 13 parallel battery pack, with and without battery thermal models

Considering the battery thermal model maybe affect the battery sizing. The performance of the designed battery pack with a thermal model in 25°C is listed in Table 6. As seen in this table, the battery pack with 13 parallel branches have about 95 km vehicle (motorcycle) range, which is lower than previous case (100 km). Therefore, the number of parallel battery branches should be resized to 14. In this case, the vehicle range would be about 101 km. The bigger battery pack (14 parallel) is more expensive in comparison with the initial design (initial and overall costs). However, both of the designed battery packs have good thermal performance (6th column of Table 6).

Table 6: The performance of the battery pack with thermal model in 25°C

Number of battery parallel	Vehicle range (km)	Initial cost (USD)	Battery life (year)	10-year overall cost (USD)	Maximum battery temperature (°C)
13	94.81	1250	5.50	2500	26.00
14	101.21	1346	5.93	2692	25.39

Fig6 shows the battery temperature rise (°C) (solid line) and tracking error (km/h) (dashed line) vs. ambient temperature for the resized pack (14 parallel branches). As seen in this figure, both of the performance is good and acceptable.

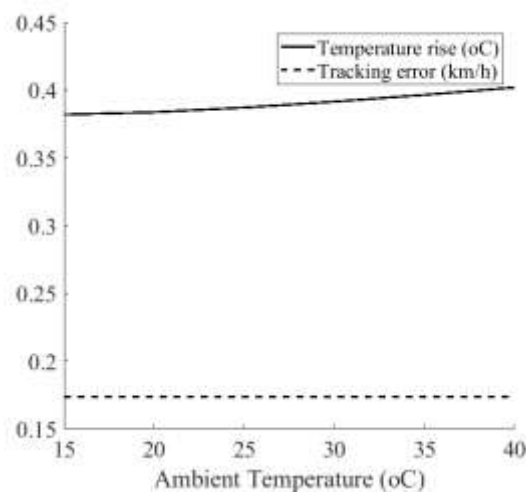


Fig6. Battery temperature rise (°C) and tracking error (km/h) vs. ambient temperature for resized pack (14 parallel branches)

Fig7 shows the vehicle (motorcycle) range (km) in different ambient temperature. As seen in this figure, the vehicle range improved with an ambient temperature rising and are higher than 100 km, except in 15°C ambient temperature. It is a reason that some of the battery thermal management systems have a warm-up subsystem for working in cold environment.

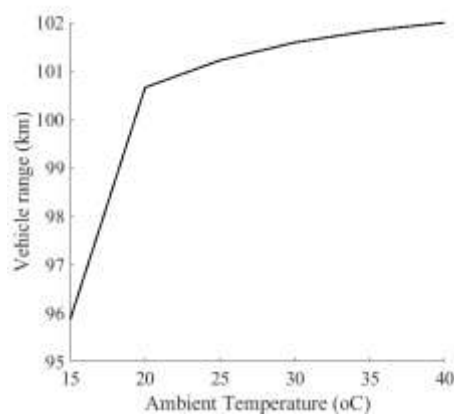


Fig7. Vehicle range (km) vs. ambient temperature for resized pack (14 parallel branches)

Fig8 shows the battery life and overall cost vs. ambient temperature for the resized battery pack (14 parallel) with a thermal model. As shown in this figure, in a warm environment (more than 25°C), the 10-year overall battery cost would be greater than 2500 USD, because the battery life is lower than five years and the battery replacement exceeds one time during ten years. This figure's trends are similar to the Fig4.

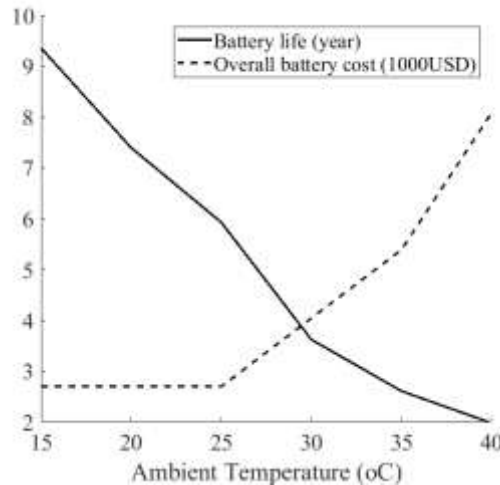


Fig8. Battery life and overall cost vs. ambient temperature for the resized battery pack (14 parallel)

4. Hybrid energy storage system

The proposed HESS in this paper is combined with a battery pack and a UC pack. The battery dynamics model is discussed in Section 2. Here, the UC model and the HESS control system is introduced.

4.1 Ultra-capacitor model

Fig9 shows the equivalent circuit model of the UC [32] in MATLAB/Simulink.

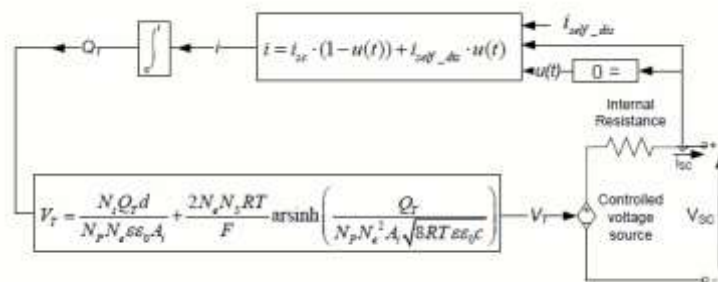


Fig9. UC dynamic model in MATLAB/Simulink [33]

The UC output voltage is calculated using a Stern equation [34] Equation (15).

$$V_{SC} = \frac{N_s Q_T d}{N_p N_e \epsilon \epsilon_0 A_i} + \frac{2 N_e N_s R T}{F} \sinh^{-1} \left(\frac{Q_T}{N_p N_e^2 A_i \sqrt{8 R T \epsilon \epsilon_0 C}} \right) - R_{SC} \cdot i_{SC} \quad (15)$$

where

$$Q_T = \int i_{SC} dt \quad (16)$$

To model the self-discharge phenomenon, the UC electric charge is corrected as equations (17) and (18) (when $i_{SC} = 0$):

$$Q_T = \int i_{self_dis} dt \quad (17)$$

$$i_{self_dis} = \begin{cases} \frac{C_T \alpha_1}{1+sR_{SC}C_T} & \text{if } t - t_{OC} \leq t_3 \\ \frac{C_T \alpha_2}{1+sR_{SC}C_T} & \text{if } t_3 \leq t - t_{OC} \leq t_4 \\ \frac{C_T \alpha_3}{1+sR_{SC}C_T} & \text{if } t - t_{OC} > t_4 \end{cases} \quad (18)$$

The parameters α_1, α_2 , and α_3 are the rates of change of the UC voltage during time intervals (t_{OC}, t_3) , (t_3, t_4) , and (t_4, t_5) respectively (Fig10).

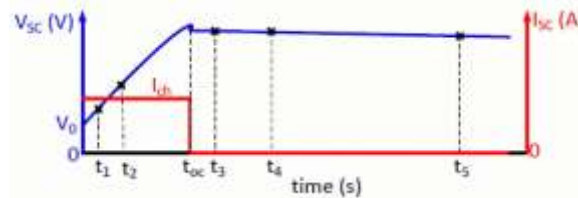


Fig10. An overview of some parameters of UC model [33]

4.2 HESS control system

The HESS configuration is “UC-battery active topology” (Fig11).

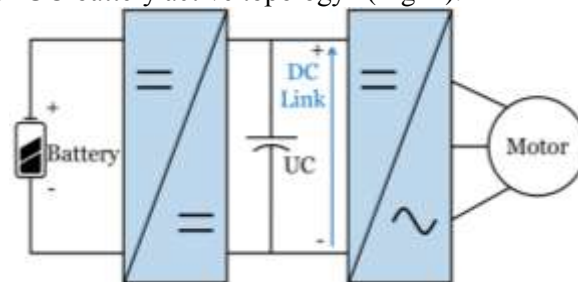


Fig11. UC-battery active topology [35]

A straightforward and powerful HESS control system, power distribution control strategy (PDCS), is used for this case study. The role of PDCS is distributing the demanded electric power between battery and UC. In the UC-based PDCS [36], the prior energy storage system is the UC, and the battery provides extra power (when the UC cannot generate all the demanded power) (Fig12).

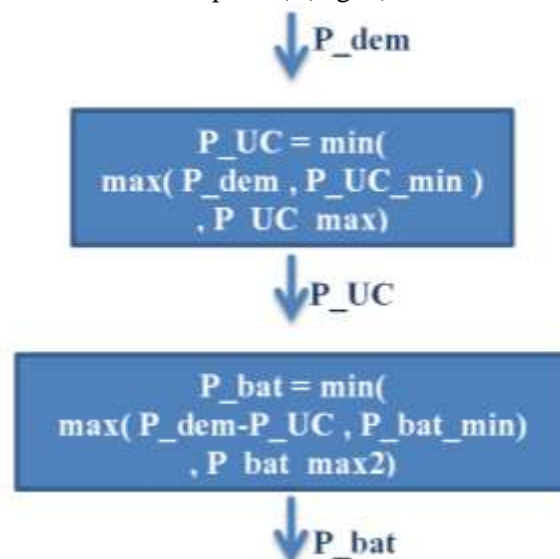


Fig12. Flowchart of the UC-based PDCS [37]

5. HESS sizing

In Table 7, the performance of HESSs with different UC capacities are listed. These results are determined without battery thermal model, and it is assumed that ambient temperature is 25°C and the battery pack has 13 parallel branches.

Table 7: The performance of different HESSs without thermal model in 25°C and 13 parallel batteries

UC capacity (F)	Tracking error (km/h)	Vehicle range (km)	Initial cost (USD)	Battery life (year)	10-year overall cost (USD)
0	0.18	99.23	1250	6.08	2500
20	0.16	94.71	1951	6.48	3201
40	0.17	96.65	2053	6.65	3303
60	0.17	97.87	2154	6.69	3404
80	0.18	98.92	2255	6.72	3505
100	0.18	94.71	2356	6.67	3606
120	0.19	95.35	2458	6.68	3708

As shown in Table 7, tracking errors (second column) are small and acceptable in all rows (every UCS), and it does not change noticeably. About vehicle range (third column), the UC adding causes to loss some fields, except in 80 F case (fifth row) which the vehicle range is near to conventional ESS. This phenomenon is related to heavier HESS pack in comparison with the standard ESS. The initial HESS costs (fourth column) are rising with UC capacity growing, same as battery life values (fifth column).

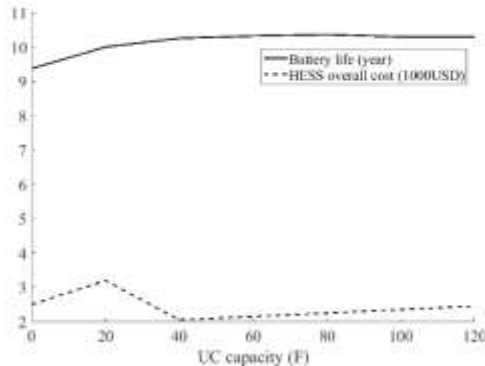


Fig13. Battery life and HESS overall cost vs. UC capacity for testing without thermal model in 15°C ambient temperature and with 13 parallel battery

Same as Table 7, the HESS performance is studied in different ambient temperature and without battery thermal model. In some environmental conditions, show that HESS overall cost is better than conventional ESS overall cost. As a sample, Fig13 shows the battery life (solid line) and HESS overall cost (dashed line) versus different UC capacities. As seen in this figure, adding UC (higher than 40 F) can reduce the HESS overall cost (because of the battery life would be over than ten years).

At a glance, suitable UC capacity for converting conventional ESS to the hybrid ESS is about 80 F, reference to the results of HESS without battery thermal model in different ambient temperature. The main UC capacity criteria are the vehicle range (e.g., Table 7 column three) and the HESS overall cost (Fig13 dashed line).

The performance of different HESSs with the thermal model are listed in Table 8. The ambient temperature is 25°C and the number of batteries in parallel is 14. The tracking errors (second column) are low and acceptable in all rows (every UCS), and it does not change noticeably, same as Table 7. In the same manner, 80 F case (fifth row) has the best solutions in sight of the vehicle range, battery life, and maximum

battery temperature. The results of the last column (maximum battery temperature) show that a HESS needs a lighter and cheaper battery thermal management system in comparison with a conventional ESS. Adding UC and lower battery current is the reason of lower battery temperature in HESS as compared with the standard ESS.

Table 8: The performance of different HESSs with thermal model in 25°C and 14 parallel batteries

UC capacity (F)	Tracking error (km/h)	Vehicle range (km)	Initial cost (USD)	Battery life (year)	10-year overall cost (USD)	Maximum battery temperature (°C)
0	0.17	101.21	1346	5.93	2692	25.45
20	0.16	95.82	2047	6.44	3394	25.25
40	0.17	97.70	2149	6.64	3495	25.19
60	0.17	98.93	2250	6.72	3596	25.17
80	0.18	99.99	2351	6.75	3697	25.16
100	0.18	95.74	2452	6.68	3799	25.17
120	0.19	96.38	2554	6.69	3900	25.17

As seen in Table 8 and mentioned before, the maximum battery temperature is reduced in HESS case in comparison with the conventional ESS. The maximum battery temperature reduction for HESS compared with the standard ESS in different ambient temperature are presented in Fig14. In this figure, the number of batteries in parallel branches are 14 and UC capacity (for HESS case) is 80 F. As shown in this figure, the HESS has better performance in higher ambient temperature for temperature reduction in comparison with lower ambient temperature. This phenomenon indicates that in warm weather, the advantages of adding UC in ESS is more noticeable, in sight of the thermal management system.

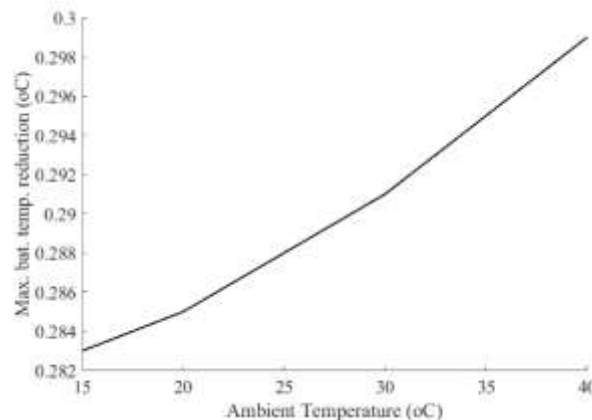


Fig14. Maximum battery temperature reduction for HESS in comparison with the conventional ESS in different ambient temperature

Fig15 shows the battery life increase for HESS compared to regular ESS in various ambient temperature; with and without battery thermal model. Same as previous cases, the number of batteries in parallel branches are 14 and UC capacity (for HESS case) is 80 F, in this figure. As shown in this figure, the UC adding has better results in lower ambient temperature for battery life increase in comparison with higher ambient temperature. Also, battery life increase with battery thermal model is higher as compared with the second case (without battery thermal model).

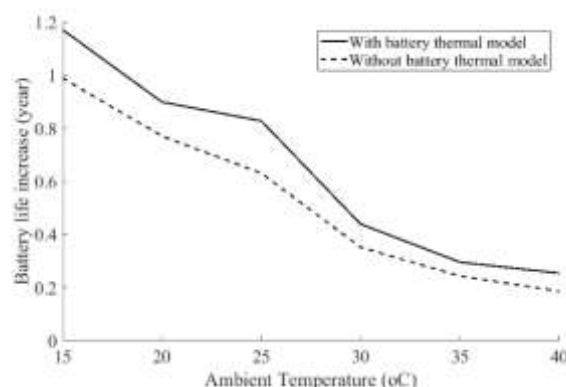


Fig15. Battery life increase for HESS in comparison with the conventional ESS in different ambient temperature; with and without battery thermal model

Fig16 shows the Battery SoC for HESS with and without battery thermal model. As seen in this figure, in thermal modeling case (more actual case) the battery SoC is lower than of the battery model without a thermal model. Therefore the effect of the thermal model should be considered for electric vehicle range calculation.

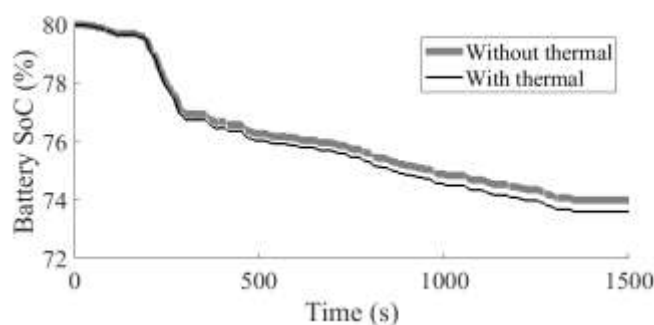


Fig16. Battery SoC for HESS with and without battery thermal model

6. Conclusion

The thermal modeling of the lithium battery is considered in this paper for studying its effect on battery and hybrid battery/ultra-capacitor sizing process for an electric vehicle. As a case study, an electric motorcycle is investigated in this research work.

The results of the conventional Energy Storage System (ESS) (battery) show that without battery thermal modeling, 13 parallel batteries are suitable for the electric motorcycle. On the other hand, with battery thermal modeling, at least 14 parallel batteries are needed to satisfy the vehicle range criterion (about 100 km) in 25°C ambient temperature. Some other outcomes, in this case, are listed below:

- Battery life is decreased when the ambient temperature growth.
- Battery temperature rise is increased when the ambient temperature growth.
- Vehicle range is increased when the ambient temperature growth.

In the Hybrid Energy Storage System (HESS) (battery/ultracapacitor) case, 80 F UC is a good sizing solution in both with and without battery thermal model. Some conclusions, in this instance, are listed below:

- As seen with battery thermal model, in HESS the maximum battery temperature is lower than a conventional ESS. Therefore, a lighter and cheaper cooling system can be used in HESS in comparison with the ESS.
- Battery life improvement for a HESS is more noticeable when the battery thermal model is used as compared with the case that the battery thermal model is disabled.

Acknowledgement

This work was supported by Automotive Engineering Research Center (AERC) of Iran University of Science and Technology (IUST).

References

- [1] R. Saneifard, R. Dana, and A. Sianati, "Design and implementation of an electromechanical system utilizing speed bumps to generate electric power," *Journal of Engineering Technology*, vol. 26, no. 2, pp. 16-23, 2009.
- [2] A. Safaei, M. R. Ha'iri-Yazdi, V. Esfahanian, M. Esfahanian, M. Masih-Tehrani and H. Nehzati, "Designing an intelligent control strategy for hybrid powertrains utilizing a fuzzy driving cycle identification agent," *Proceedings of the Institution of Mechanical Engineers, Part D: Journal of Automobile Engineering*, vol. 229, no. 9, pp. 1169-1188, 2015.
- [3] P. Ahmadizadeh and B. Mashadi, "Power flow and efficiency analysis of the EM power split mechanism," *Journal of the Brazilian Society of Mechanical Sciences and Engineering*, vol. 39, no. 6, pp. 1947-1955, 2017.
- [4] A. Mahmoudzadeh Andwari, A. Pesiridis, S. Rajoo, R. Martinez-Botas and V. Esfahanian, "A review of Battery Electric Vehicle technology and readiness levels," *Renewable and Sustainable Energy Reviews*, vol. 78, pp. 414-430, 2017.
- [5] A. Sharma and V. Strezov, "Life cycle environmental and economic impact assessment of alternative transport fuels and power-train technologies," *Energy*, vol. 133, pp. 1132-1141, 2017.
- [6] Y. Gao, J. Jiang, C. Zhang, W. Zhang, Z. Ma and Y. Jiang, "Lithium-ion battery aging mechanisms and life model under different charging stresses," *Journal of Power Sources*, vol. 356, pp. 103-114, 2017.
- [7] T. Xian, C. Soon, S. Rajoo and A. Romagnoli, "A parametric study: The impact of components sizing on range extended electric vehicle's driving range," in *2016 Asian Conference on Energy, Power and Transportation Electrification (ACEPT 2016)*, Singapore, Singapore, 2017.
- [8] T. Markel, A. Brooker, T. Hendricks, V. Johnson, K. Kelly, B. Kramer, M. O'Keefe, S. Sprick and K. Wipke, "ADVISOR: A systems analysis tool for advanced vehicle modeling," *Journal of Power Sources*, vol. 110, no. 1, pp. 255-266, 2002.
- [9] F. Sangtarash, V. Esfahanian, H. Nehzati, S. Haddadi, M. Bavanpour and B. Haghpanah, "Effect of different regenerative braking strategies on braking performance and fuel economy in a hybrid electric bus employing cruise vehicle simulation," *SAE International Journal of Fuels and Lubricants*, vol. 1, no. 1, pp. 828-837, 2009.
- [10] M. Esfahanian, A. Safaei, H. Nehzati, V. Esfahanian and M. Masih-Tehrani, "Matlab-based modeling, simulation and design package for Electric, Hydraulic and Flywheel hybrid powertrains of a city bus," *International Journal of Automotive Technology*, vol. 15, no. 6, pp. 1001-1013, 2014.
- [11] H. He, R. Xiong and J. Fan, "Evaluation of lithium-ion battery equivalent circuit models for state of charge estimation by an experimental approach," *Energies*, vol. 4, no. 4, pp. 582-598, 2011.
- [12] O. Tremblay and L. Dessaint, "Experimental validation of a battery dynamic model for EV applications," *World Electric Vehicle Journal*, vol. 3, no. 1, pp. 1-10, 2009.
- [13] K. Smith and C.-Y. Wang, "Power and thermal characterization of a lithium-ion battery pack for hybrid-electric vehicles," *Journal of Power Sources*, vol. 160, no. 1, pp. 662-673, 2006.
- [14] K. Marr, V. Somandepalli and Q. Horn, "Explosion hazards due to failures of lithium-ion batteries," in *2013 AIChE Spring Meeting and 9th Global Congress on Process Safety (AIChE 2013)*, San Antonio (USA), 2013.
- [15] S. Janarthanam, N. Burrows and B. Boddakayala, "Factors Influencing Liquid over Air Cooling of High Voltage Battery Packs in an Electrified Vehicle," in *SAE World Congress Experience (WCX 2017)*, Detroit (USA), 2017.
- [16] C. Arapatsakos, K. Galanopoulos and T. Koutroumanidis, "Catalyst temperature difference in relation to carbon monoxide emissions in a four-stroke engine," *Journal of Engineering Technology*, vol. 21, no. 2, pp. 52-55, 2004.

- [17] P. Nelson, R. Vijayagopal, K. Gallagher and A. Rousseau, "Sizing the battery power for PHEVs based on battery efficiency, cost and operational cost savings," *World Electric Vehicle Journal*, vol. 6, no. 3, pp. 514-522, 2013.
- [18] P. Correa, D. Fernandez, M. Gaudiano, L. Mathe, E. Moschen and P. Munoz, "Sizing and optimal energy management in an electric vehicle with fuel cell using dynamic vehicle models," in 2nd IEEE Biennial Congress of Argentina (ARGENCON 2014), San Carlos de Bariloche (Argentina), 2014.
- [19] F. Colzi, M. De Nigris, A. Corti and S. Savaresi, "Extended range electric vehicles components preliminary sizing based on real mission profiles," in 27th World Electric Vehicle Symposium and Exhibition (EVS 2014), Barcelona (Spain), 2013.
- [20] L. Malesani, L. Rossetto and P. Tenti, "Active power filter with hybrid energy storage," in 20th Annual IEEE Power Electronics Specialists Conference (PESC'89), Milwaukee, WI, USA, 1989.
- [21] X. Wu, X. Hu, Y. Teng, S. Qian and R. Cheng, "Optimal integration of a hybrid solar-battery power source into smart home nanogrid with plug-in electric vehicle," *Journal of Power Sources*, vol. 363, no. 30 September 2017, pp. 277-283, 2017.
- [22] M. Ruiz-Cortés, E. Romero-Cadaval, C. Roncero-Clemente, F. Barrero-Gonzalez and E. Gonzalez-Romera, "Energy management strategy to coordinate batteries and ultracapacitors of a hybrid energy storage system in a residential prosumer installation," in 2017 International Young Engineers Forum (YEF-ECE 2017), Tryp Lisboa Caparica Mar HotelCaparica (Portugal), 2017.
- [23] R. Bartholomäus, T. Lehmann and U. Schneider, "Model predictive control of highly efficient dual mode energy storage systems including DC/DC converter," in SpringerBriefs in Applied Sciences and Technology, Berlin (Germany), Springer Verlag, 2018, pp. 33-46.
- [24] S. M. Lukic, J. Cao, R. C. Bansal, F. Rodriguez and A. Emadi, "Energy storage systems for automotive applications," *IEEE Transactions on industrial electronics*, vol. 55, no. 6, pp. 2258-2267, 2008.
- [25] M. Masih-Tehrani, M.-R. Ha'iri-Yazdi, V. Esfahanian and H. Sagha, "Development of a hybrid energy storage sizing algorithm associated with the evaluation of power management in different driving cycles," *Journal of Mechanical Science and Technology*, vol. 26, no. 12, pp. 4149-4159, 2012.
- [26] Mathworks, "Implement generic battery model," 2017. [Online]. Available: <https://www.mathworks.com/help/physmod/sps/powersys/ref/battery.html>.
- [27] L. S. K. Saw, Y. Ye and A. Tay, "Electro-thermal analysis of Lithium Iron Phosphate battery for electric vehicles," *Journal of Power Sources*, vol. 249, pp. 231-238, 2014.
- [28] N. Omar, M. Monem, Y. Firouz, J. Salminen, J. Smekens, O. Hegazy, H. Gaulous, G. Mulder, P. Van den Bossche, T. Coosemans and J. Van Mierlo, "Lithium iron phosphate based battery — Assessment of the aging parameters and development of cycle life model," *Applied Energy*, vol. 113, no. January 2014, p. 1575–1585, 2014.
- [29] J. Wang, P. Liu, J. Hicks-Garner, E. Sherman, S. Soukiazian, M. Verbrugge and P. Finamore, "Cycle-life model for graphite-LiFePO₄ cells," *Journal of Power Sources*, vol. 196, no. 8, pp. 3942-3948, 2011.
- [30] M. Masih-Tehrani, M. R. Ha'iri-Yazdi, V. Esfahanian and A. Safaei, "Optimum sizing and optimum energy management of a hybrid energy storage system for lithium battery life improvement," *Journal of Power Sources*, vol. 244, pp. 2-10, 2013.
- [31] M. Montazeri-Gh and M. Naghizadeh, "Development of car drive cycle for simulation of emissions and fuel economy," in Proceedings of 15th European simulation symposium, Delft, The Netherlands, 2003.
- [32] N. Xu and J. Riley, "Nonlinear analysis of a classical system: The double-layer capacitor," *Electrochemistry Communications*, vol. 13, no. 10, pp. 1077-1081, 2011.
- [33] Mathworks, "Implement generic supercapacitor model," 2017. [Online]. Available: <https://www.mathworks.com/help/physmod/powersys/ref/supercapacitor.html>.
- [34] K. B. Oldham, "A Gouy–Chapman–Stern model of the double layer at a (metal)/(ionic liquid) interface," *Journal of Electroanalytical Chemistry*, vol. 613, no. 2, pp. 131-138, 2008.
- [35] E. Chemali, M. Preindl, P. Malysz and A. Emadi, "Electrochemical and electrostatic energy storage and management systems for electric drive vehicles: State-of-the-art review and future trends.," *IEEE Journal of Emerging and Selected Topics in Power Electronics*, vol. 4, no. 3, pp. 1117-1134, 2016.

- [36] Z. Amjadi and S. S. Williamson, "Power-electronics-based solutions for plug-in hybrid electric vehicle energy storage and management systems," *IEEE Transactions on Industrial Electronics*, vol. 57, no. 2, pp. 608-616, 2010.
- [37] M. Masih-Tehrani, M. Hairi-Yazdi and V. Esfahanian, "Power Distribution Development and Optimization of Hybrid Energy Storage System," *International Journal of Automotive Engineering*, vol. 4, no. 2, pp. 675-684, 2014.
- [38] C. Zhu, X. Li, L. Song and L. Xiang, "Development of a theoretically based thermal model for lithium ion battery pack," *Journal of Power Sources*, vol. 223, p. 155–164, 2013.
- [39] O. Tremblay and L.-A. Dessaint, "Experimental validation of a battery dynamic model for EV applications," *World Electric Vehicle Journal*, vol. 3, no. 1, 2009.